applied sciences

MDPI

Article

# Magnetic Field Effect of Near-Field Radiative Heat Transfer for SiC Nanowires/Plates

**Zhiyuan Shen [1], Hao Wu [2] and Han Wang [2,*]**

[1] College of Civil Aviation, Nanjing University of Aeronautics and Astronautics, Nanjing 210016, China; shenzy@nuaa.edu.cn

[2] School of Energy Science and Engineering, Nanjing Tech University, Nanjing 211800, China; wuhaodlgc@njtech.edu.cn

* Correspondence: wangh_njt@njtech.edu.cn

Received: 17 September 2018; Accepted: 20 October 2018; Published: 23 October 2018


**Abstract:** The SiC micro/nano-scale structure has advantages for enhancing nonreciprocal absorptance for photovoltaic use due to the magneto optical effect. In this work, we demonstrate the near-field radiative transfer between two aligned SiC nanowires/plates under different magnetic field intensities, in which Lorentz-Drude equations of the dielectric constant tensor are proposed to describe the dielectric constant as a magnetic field applied on the SiC structure. The magnetic field strength is qualified in this study. Using local effective medium theory and the fluctuation-dissipation theorem, we evaluate the near-field radiation between SiC nanowires with different filling ratios and gap distances under an external magnetic field. Compared to the near-field heat flux between two SiC plates, the one between SiC nanowires can be enhanced with magnetic field intensity, a high filling ratio, and a small gap distance. The electric field intensity is also presented for understanding light coupling, propagation, and absorption nature of SiC grating under variable incidence angles and magnetic field strengths. This relative study is useful for thermal radiative design in optical instruments.

**Keywords:** magnetic field effect; near-field radiation; SiC nanowires

## 1. Introduction

When the distance between two materials is less than the thermal characteristic wavelength, also known as the characteristic wavelength of thermal radiation, evanescent waves play a dominant role in radiative heat transfer. The energy transfer can be further enhanced and Plank's theory of thermal radiation is no longer valid, which is called near-field radiative heat transfer [1–4]. At nanometer distances, near-field radiative heat transfer can be several orders of magnitude greater than that between two far field blackbodies, especially when surface plasmon polaritons (SPPs) or surface phonon polaritons (SPhPs) are excited [5–9]. Due to the advent of near field radiative heat transfer and its wide potential applications in micro- and nano-scale thermophotovoltaic (TPV) cells, thermal imaging and local thermal management, near-field radiative heat transfer had attracted significant attention [10–17].

Some researchers have found that applying an external magnetic field to a semiconductor causes some changes in its optical properties. Under the action of a magnetic field, the atoms, or ions within the intrinsic magnetic moment material, produce magnetic induction phenomenon, resulting in the orderly arrangement of the magnetic moment, which affects the transmission of light in its internal features, called the magneto-optical effect. This effect can break the time reversal invariance of the quantum mechanics of materials, and the Kirchhoff's law is no longer valid [18–20]. Wu et al. [21] discovered the near-field radiative characteristics of magneto dielectric uniaxial anisotropic media (MDUAM)

that have both magnetic and electric anisotropy. However, the above works all focused on near-field radiative heat transfer (NFRHT) for homogeneous isotropic media. Then, Song et al. [22] studied the NFRHT between graphene and anisoropic magneto-dielectric hyperbolic metamaterials (AMDHMs) according to the fluctuational dissipation theorem. They found that extraordinary propagating modes enable the total NFRHT flux to exceed that between graphene and SiC nanowires by several fold. Although the above research considered the impact of magnetic permeability, the effect of the magnetic field was lacking the MDUAM and AMDHMs were all ideal models, and the magnetic field strength was not quantified.

SiC is a widely used semiconductor that can be manufactured as optical control elements, such as wavelength-selective photodetectors, photovoltaic cells, and absorbers. Few studies of NFRHT for SiC have been conducted, and most studies investigated the SPhP coupling of SiC . Basu et al. [23] theoretically investigated the improvement of near-field radiative transfer between SiC plates due to strong SPhPs coupling. Yue et al. [24] studied the effect of magnetic polaritons (MPs) inside the SiC grating microstructures on near-field radiative transfer. The presented MPs greatly affected the spectral heat flux beside the SPhPs. However, the above works all focused on near-field radiative transfer for reciprocal materials, lacking studies on effect of non-reciprocal materials as magneto-optical materials. Hence, we investigated the non-reciprocal effect between magneto-optical materials under near-field in order to explore new phenomena.

In a previous study, the optical characteristics of the magneto-optical materials, such as SiC, InSb, and HgCdTe, was examined as an external magnetic field was applied, and a detailed description of the dielectric constant was verified and provided [25,26]. In this work, we theoretically calculate the near field radiative transfer based on SiC nanowires with different filling ratios and gap distances under an external magnetic field by using fluctuation-dissipation theorem and local effective medium theory (EMT), in which Lorentz-Drude equations of dielectric constant tensor are proposed to describe the dielectric constant as a magnetic field is applied toon the SiC. The influence of magnetic field intensity on the near field thermal radiation for SiC nanowires and plates is quantified discussed in detail. We also analyzed the influence of magnetic field intensity on the near field thermal radiation of SiC nanowires/plates.

## 2. Theoretical Formulation

### *2.1. Geometry and Radiative Properties of SiC Nanowires*

The emitter and receiver temperatures were respectively set as $T_1$ = 300 K and $T_2$ = 299 K in this work. From Figure 1, we can see that the vacuum gap distance is denoted as $d$. Note that the maximum $f$ for aligned SiC nanowires is 0.3 due to using the approximation Maxwell Garnet method, which is suitable for a dilute system. The dielectric constant of SiC is described by the Lorentz-Drude model as: [27]

$$\varepsilon_{(\omega)} = \varepsilon_\infty \left( 1 + \frac{\omega_p^2}{\omega_T^2 - \omega^2 - i\gamma\omega} \right) \tag{1}$$

where $\varepsilon_\infty$ is the high-frequency limit permittivity ($\varepsilon_\infty$ = 6.38), $\omega_T$ is the angular frequency of the incident wave ($\omega_T = 1.50 \times 10^{14}$ rad/s), $\gamma$ is the collision frequency of free electrons ($\gamma = 1/\tau$, $\tau$ is relaxation time) and $\gamma = 4 \times 10^{11}$ rad/s, and $\omega_p = \sqrt{Ne^2/\varepsilon_0 m^*}$ is the plasma frequency in rad/s.

In this paper, only the magnetization vector M parallel to the $Z$ axis is considered. When the magnetic field H is perpendicular to the plane of incidence (i.e., p-polarized or Transverse Magnetic (TM) waves), medium 2 cannot be simply treated as an isotropic medium because the electric field and

the optical axis form an acute angle. Hence, for anisotropic materials, the permittivity tensor under a magnetic field can be expressed as:

$$\bar{\varepsilon} = \begin{pmatrix} \varepsilon_{xx} & \varepsilon_{xy} & 0 \\ -\varepsilon_{xy} & \varepsilon_{yy} & 0 \\ 0 & 0 & \varepsilon_{zz} \end{pmatrix} \tag{2}$$

To simplify the complexity of the computation, a unitary matrix transformation U is used to diagonalize the permittivity, as shown below, by treating the anisotropic dielectric tensor as being plane symmetric. The approximate dielectric constant can be expressed as:

$$\bar{\varepsilon}_D = \mathrm{U}^* \cdot \bar{\varepsilon} \cdot \mathrm{U} = \begin{pmatrix} \varepsilon_{xx} & 0 & 0 \\ 0 & \varepsilon_{yy} & 0 \\ 0 & 0 & \varepsilon_{zz} \end{pmatrix} = \begin{pmatrix} n_{xx}^2 & 0 & 0 \\ 0 & n_{yy}^2 & 0 \\ 0 & 0 & n_{zz}^2 \end{pmatrix} \tag{3}$$

So, the dielectric constant tensor of SiC can be expressed as [24]:

$$\bar{\varepsilon} = \begin{pmatrix} \varepsilon_\infty\left(1 - \frac{\omega_p^2(\omega+\gamma i)}{\omega\left[(\omega+\gamma i)^2-\omega_c^2\right]-\omega_T^2(\omega+\gamma i)}\right) & \frac{i\omega_p^2\omega_c}{\omega\left[(\omega+\gamma i)^2-\omega_c^2\right]-\omega_T^2(\omega+\gamma i)} & 0 \\ -\frac{i\omega_p^2\omega_c}{\omega\left[(\omega+\gamma i)^2-\omega_c^2\right]-\omega_T^2(\omega+\gamma i)} & \varepsilon_\infty\left(1 - \frac{\omega_p^2(\omega+\gamma i)}{\omega\left[(\omega+\gamma i)^2-\omega_c^2\right]-\omega_T^2(\omega+\gamma i)}\right) & 0 \\ 0 & 0 & \varepsilon_\infty\left(1 - \frac{\omega_p^2}{\omega_T^2-\omega^2-i\gamma\omega}\right) \end{pmatrix} \tag{4}$$

The doping concentration can be expressed as $N = aT^{3/2}\exp(-E_g/2kT)$, $a$ is a coefficient related material, the Boltzmann constant $k$ = 8.625 × $10^{-5}$ eV/$k$, $E_g$ = 2.2 eV is the energy gap in eV, $T$ is the temperature which the structure operates, $e$ = 1.6 × $10^{19}$ C is the elementary charge, and $\varepsilon_0$ = 8.85 × $10^{-12}$ is the free-space permittivity in $c^2/m^2N$. The cyclotron frequency follows $\omega_c = eB/m^*$, where $B$ refers to the applied field intensity. So the doping concentration was calculated as $N$ = 3.7 × $10^{23}$ $m^{-3}$.

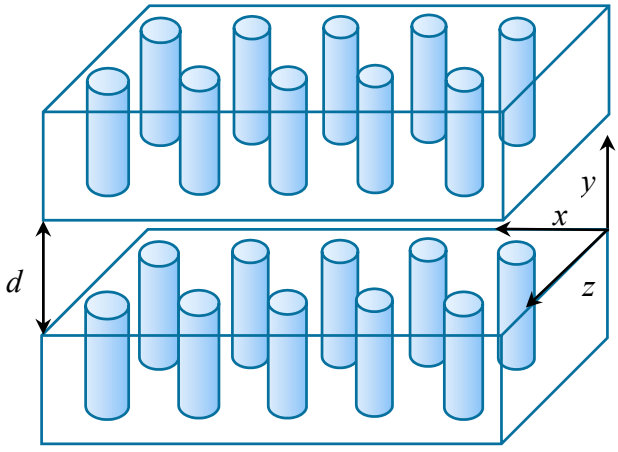


**Figure 1.** Schematic of radiative heat transfer between two-infinite SiC nanowires separated by a vacuum gap $d$.

In Figure 2, the dielectric constants of SiC are plotted as a real part and imaginary part, respectively for $B$ = 0 T and $B$ = 3 T. From Figure 2, the results of the Lorentz-Drude model for both real and imaginary parts agree well with data reported by Palik [27]. The real part increases as the angular frequency increases, which shows the usual dispersion characteristics, and decreases as the angular frequency increases, showing a unusual dispersion characteristics. The imaginary part showed a similar trend. Hence, the Lorentz-Drude model is suitable to calculate the dielectric constant of SiC.

As the magnetic field was applied, the real and imaginary part had obvious oscillation as shown in Figure 2b, as the magnetic field affected the optical constant of SiC.

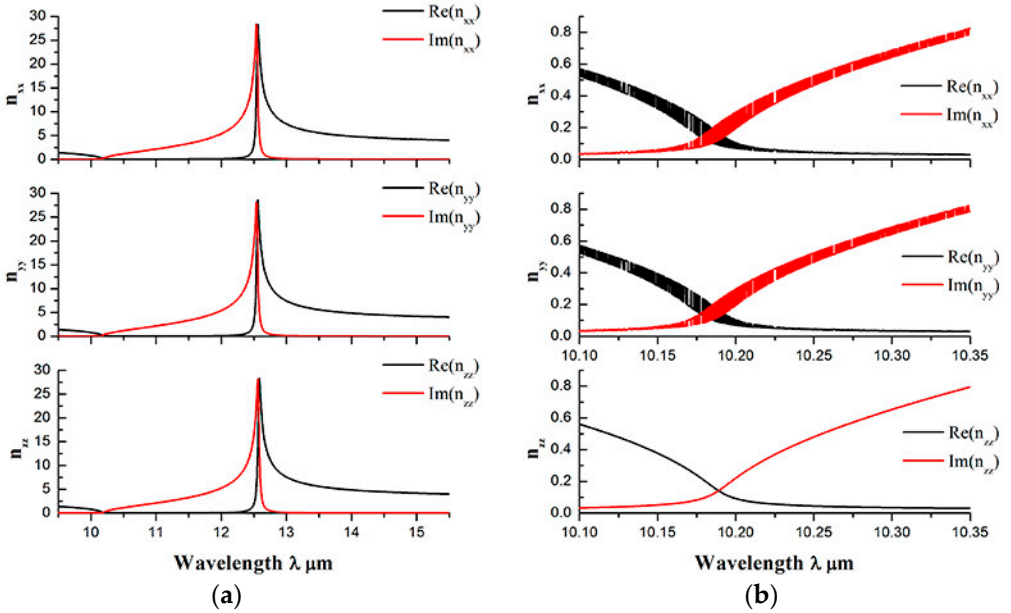


**Figure 2.** Equivalent refractive index $n$ of SiC under magnetic field (**a**) $B$ = 0 T, (**b**) $B$ = 3 T.

In general, the application of a magnetic field somewhat affects the optical constant of SiC, especially in the $x$ and $y$ directions.

### 2.2. *Effective Medium Theory*

Local effective medium theory (EMT) was used to obtain the anisotropic dielectric function and was combined with fluctuation electrodynamics to calculate the near-field radiative heat transfer coefficient due to its simplicity and low computational demand. In the Maxwell-Garnett approximation, the effective properties of a composite medium are obtained by treating one constituent of the composite as the host and all other constituents as embedded fillers that are not in contact with one another [28].

For SiC nanowire arrays, we set the optical axis of the structure along the $Z$ axis, and obtained the effective dielectric functions:

$$\varepsilon_{x,y} = \frac{\bar{\varepsilon}_{x,y}(1+f)+(1-f)}{\bar{\varepsilon}_{x,y}(1-f)+(1+f)} \tag{5}$$

$$\varepsilon_z = \bar{\varepsilon}_z f + 1 - f \tag{6}$$

EMT is a homogenization method for characterizing the optical properties of an inhomogeneous medium with different material constituents based on the field average method. In Equations (5) and (6), $f$ means the volume filling ratio, which has been previously explained in detail [27].

Form Figure 3, the hyperbolic dispersions of SiC nanowires under magnetic field $B$ = 3 T were supported in two narrow bands between $1.50 \times 10^{14}$ rad/s and $1.69 \times 10^{14}$ rad/s (blue shaded region, Type I), and between $1.79 \times 10^{14}$ rad/s and $1.83 \times 10^{14}$ rad/s (yellow shaded region, Type II). The heat transfer coefficient at temperature $T$ between two semi-infinite plates can be expressed as:

$$H = \frac{1}{8\pi^3}\int_0^\infty \Theta(\omega,T)d\omega \int_0^{2\pi}\int_0^\infty \xi(\omega,\beta,\phi)\beta d\beta d\phi \tag{7}$$

where $\Theta(\omega,T) = \frac{\partial}{\partial T}(\hbar\omega/(\exp(\hbar\omega/k_BT)-1))$ is the average energy of a Planck's oscillator, $\hbar$ is the reduced Planck constant, $\beta$ is the transverse wavevector (the magnitude of the wavevector component

in the $x-y$ plane), $\phi$ is the Azimuth of a wavevector, and $\xi(\omega,\beta,\phi)$ is the energy transmission coefficient, which can be defined as:

$$\xi(\omega,\beta,\phi)=\begin{cases}\mathrm{Tr}[(\mathrm{I}-\mathrm{R}_2^*\mathrm{R}_2)\mathrm{D}(\mathrm{I}-\mathrm{R}_1\mathrm{R}_1^*)\mathrm{D}^*], & \beta<k_0\\ \mathrm{Tr}[(\mathrm{R}_2^*-\mathrm{R}_2)\mathrm{D}(\mathrm{R}_1-\mathrm{R}_1^*)\mathrm{D}^*]e^{-2|\mathrm{k}_{y0}|d}, & \beta>k_0\end{cases} \tag{8}$$

Here, the matrix D is expressed as $\mathrm{D}=\left(\mathrm{I}-\mathrm{R}_1\mathrm{R}_2e^{2ik_{y0}d}\right)^{-1}$, I is a $2\times2$ unit matrix, R is the matrix related to Fresnel's reflection coefficients and

$$\mathrm{R}_{1,2}=\begin{bmatrix}r_{ss}^{(1,2)} & r_{sp}^{(1,2)}\\ r_{ps}^{(1,2)} & r_{pp}^{(1,2)}\end{bmatrix} \tag{9}$$

where $j$ is for $s$ or $p$ polarization, and $\gamma$ is Fresnel coefficient, which can be expressed as follows:

$$r_j=\begin{cases}\dfrac{k_{y0}-\sqrt{k_0^2\varepsilon_x-\beta^2}}{k_{y0}+\sqrt{k_0^2\varepsilon_x-\beta^2}}, j=s\\ \dfrac{\varepsilon_x k_{y0}-\sqrt{k_0^2\varepsilon_x-\beta^2\varepsilon_x/\varepsilon_y}}{\varepsilon_x k_{y0}+\sqrt{k_0^2\varepsilon_x-\beta^2\varepsilon_x/\varepsilon_y}}, j=p\end{cases} \tag{10}$$

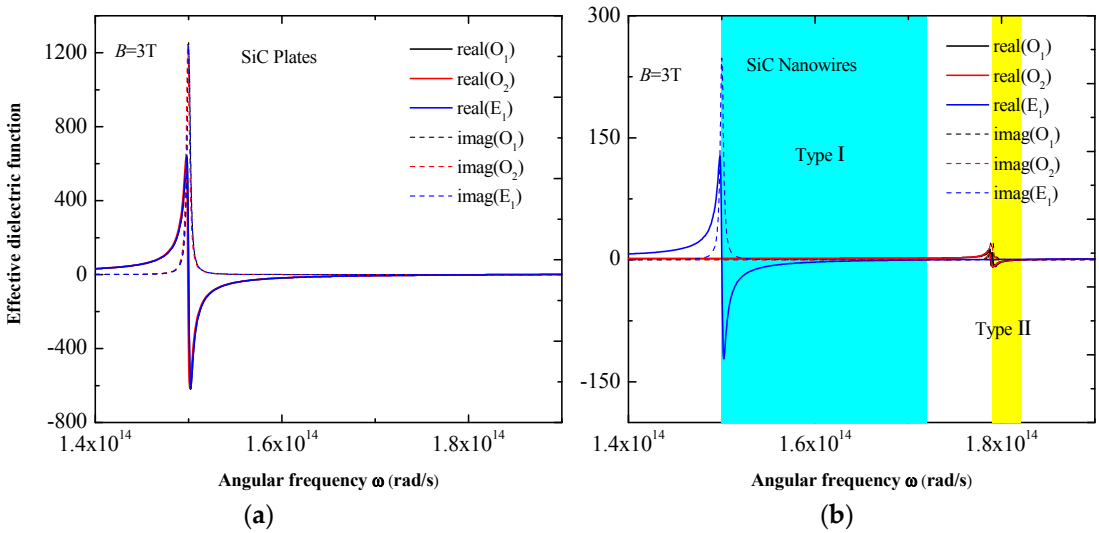


**Figure 3.** The effective dielectric function for (**a**) SiC plates and (**b**) SiC nanowires at $f$ = 0.2.

In order to check the reliability of the above model for near-thermal radiation, the heat transfer coefficient was calculated and compared to that obtained by Liu et al. [29] for doped Si nanowires and nanoholes, which is shown in Figure 4. The doping concentration was set to $N = 10^{20}$ cm$^{-3}$.

From Figure 4, the results for the two nanostructures agree well. Hence, we assumed that the above model in this work is reliable. Note that no magnetic field was applied in this case. The calculated heat transfer coefficient between doped Si nanowires with $f$ = 0.05 was 6.25 W/m$^2$K and that between doped Si nanoholes with $f$ = 0.3 was 3.83 W/m$^2$K, which are basically the same values reported in the literature.

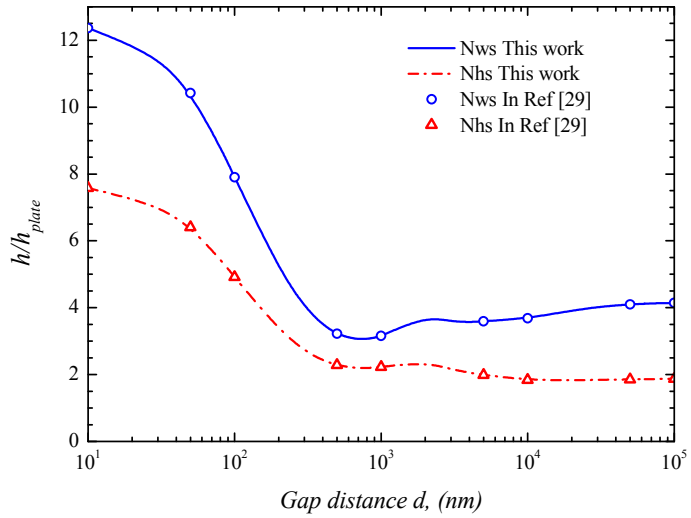


**Figure 4.** Comparison of the heat transfer coefficient in this work with that in Liu et al. [29].

## 3. Results and Discussion

### *3.1. Spectral Heat Fluxes and Transmission Coefficient*

From Figure 5, for the plate case, two peaks were observed at frequencies around $1.50 \times 10^{14}$ rad/s and $1.81 \times 10^{14}$ rad/s under $B = 3$ T. Compared to the plate case, a significantly enhanced spectral heat flux between $1.50 \times 10^{14}$ rad/s and $1.70 \times 10^{14}$ rad/s was observed, which is known as hyperbolic dispersion (Type I, blue region). Between $1.70 \times 10^{14}$ rad/s and $1.90 \times 10^{14}$ rad/s, the peak of spectral heat flux blueshifted toward increasing angular frequency, because the optical constants change due to different material structures. The linear shape of the spectral heat flux of the nanowires was obviously higher than that of the plates, producing violent shocks under the external magnetic field (Type II, yellow region).

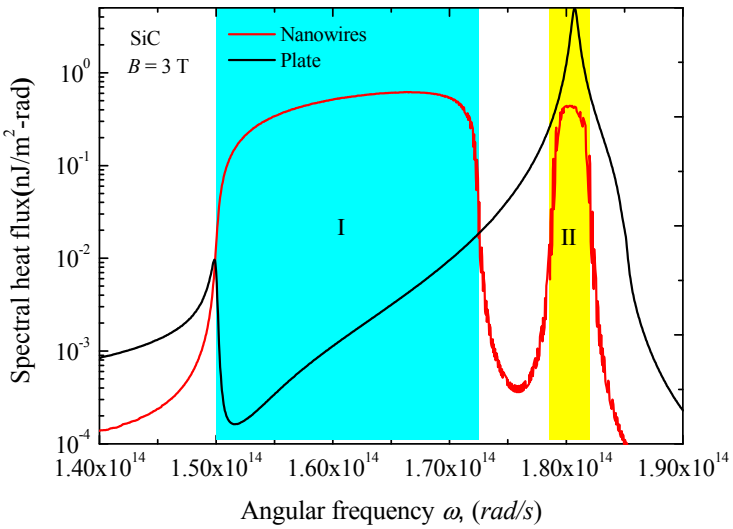


**Figure 5.** Spectral heat fluxes between two aligned SiC nanowires and between two SiC plates with $f$ = 0.2 at $d$ = 10 nm.

Figure 5 shows that compared to hyperbolic dispersion type II, SiC nanowires exhibit large heat transfer flux in the hyperbolic dispersion type I region. Compared to the SiC plates, the spectral heat flux of the nanowires structure is more intense, especially in the hyperbolic dispersion regions.

Figure 6 displays the contour plots of the transmission coefficient for both SiC nanowires and SiC plates under the magnetic field $B$ = 3 T at $d$ = 10 nm. Compared to SiC plates, the transmission coefficient of SiC nanowires is higher at very large $\beta$ values and in the hyperbolic band. This can allow photons on the surface of SiC nanowires to tunnel through the vacuum gap, which is why the heat fluxes of SiC nanowires is obviously higher than that of the plates in the hyperbolic band. Evanescent waves are the main surface mode of structure in this case. For SiC nanowires, because of their dielectric anisotropy, they support the hyperbolic band for $p$ polarization. Therefore, in the hyperbolic regions, the nanowires can have a larger transmission coefficient than that of SiC plates.

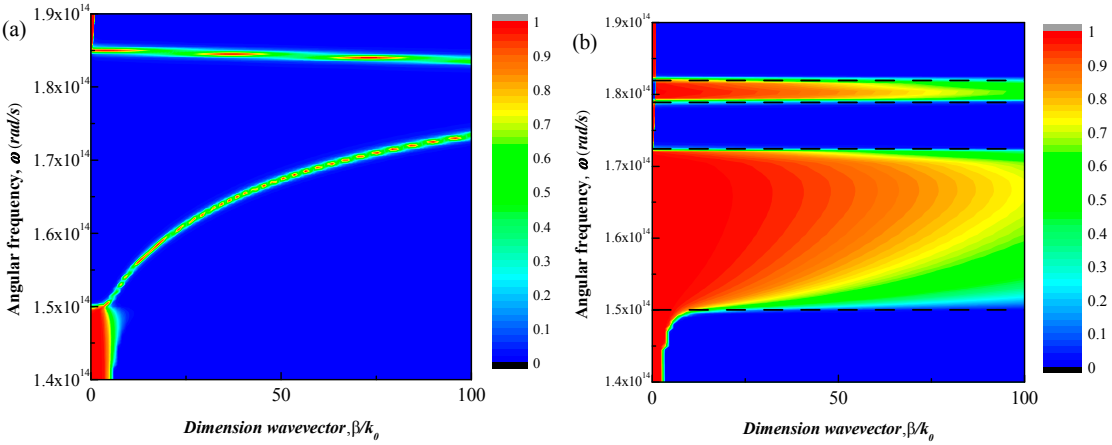


**Figure 6.** Contour of the transmission coefficient for (**a**) SiC plates and (**b**) SiC Nanowires at $d$ = 10 nm.

## 3.2. *Effect of Structure Parameters*

### 3.2.1. Filling Ratio

The filling ratio $f$ is defined based on the volume fraction of SiC. The heat transfer coefficients for SiC nanowires under different magnetic field intensities at $d$ = 10 nm were simulated as plotted in Figure 7. Note that the maximum filling ratio for the nanowires was 0.3.

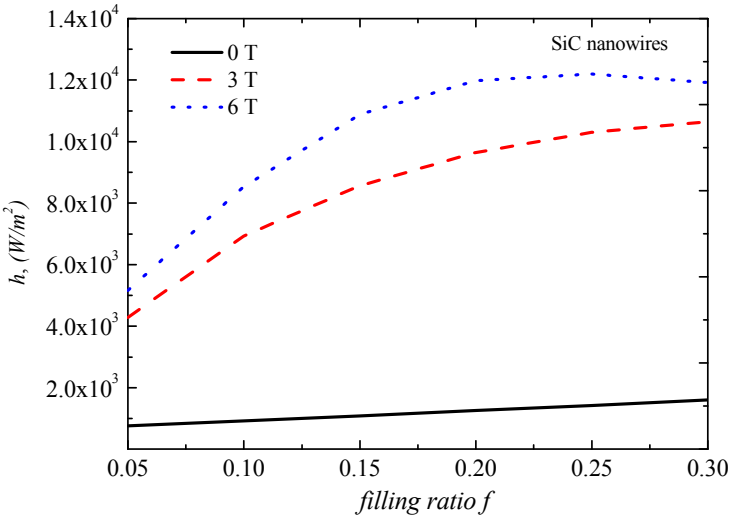


**Figure 7.** Heat transfer coefficient versus filling ratio of nanowires at a gap distance $d$ = 10 nm.

From Figure 7, we found that the heat transfer coefficient of the nanowire structure obviously increased with increasing magnetic field. This is because the magnetic field leads to a significant increase in the photon tunneling phenomenon of the material structure. The SiC plates are not

shown here because they remained constant and slightly changed as the external magnetic field strength increased.

#### 3.2.2. Gap Distance

Figure 8 shows the heat transfer coefficient between SiC nanowires at several different vacuum gap distances. For SiC plates, the heat transfer coefficient of the plate under different magnetic field intensities did not change significantly at all gap distances. Hence, it is not shown here. This occurred because the dielectric constant of the SiC plates under the action of an external magnetic field had no obvious change, as shown in Figure 3.

For $f$ = 0.2, SiC nanowires can yield a super-Planckian behavior when the gap distance is below 3 μm, whereas the heat transfer coefficient decreases with increasing gap distance. The heat transfer coefficient of the structure under a magnetic field was significantly higher than that of non-magnetic field when $d$ was below 100 nm. The enhanced amplitude increased with increasing magnetic field intensity and decreasing gap distance. Evanescent waves were the main surface mode of the structure in this case. Therefore, the external magnetic field can significantly enhance evanescent waves in near field thermal radiation.

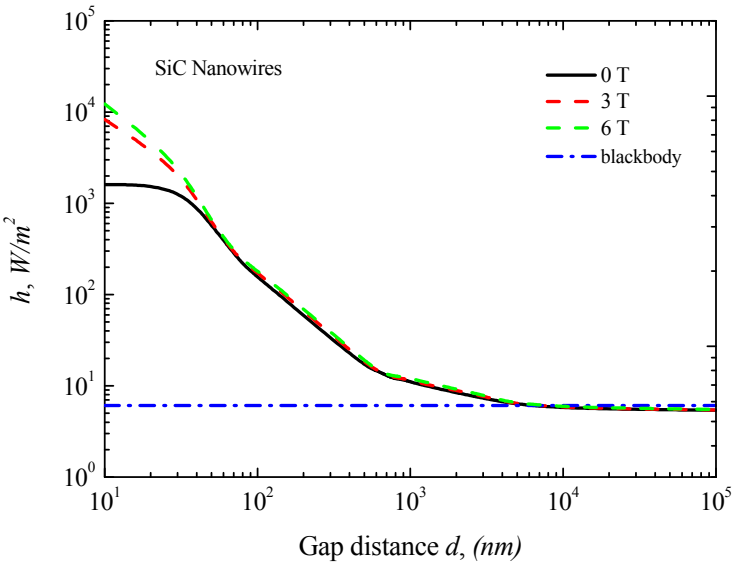


**Figure 8.** Heat transfer coefficient versus gap distance and a filling ratio of 0.2.

## 4. Conclusions

In this paper, we determined the radiative transfer properties of SiC nanowires under different external magnetic field intensities, such as spectral heat fluxes, transmission coefficient, and heat transfer coefficient, and theoretically investigated the effect of an external magnetic field on the SiC nanowires on near field thermal radiative transfer. Compared to SiC plates, the transmission coefficient of SiC nanowires was higher at very large lateral wavevector values and in the hyperbolic band. In general, the external magnetic field tunes the near field radiation properties of the subwavelength magneto-optical materials. Under the appropriate parameters, external magnetic fields obviously enhance the evanescent waves in near field thermal radiation. In summary, the external magnetic field's effect on SiC nanowires in near field heat radiation has important applications like thermophotovoltaic energy conversion and radiation-based thermal management.

**Author Contributions:** Conceptualization and Methodology, H.W. (Han Wang); Software, Validation, and Data Curation, Z.S.; Formal Analysis, Investigation, H.W. (Hao Wu); Writing-Original Draft Preparation, Z.S.; Writing-Review & Editing, H.W. (Han Wang); Visualization, H.W. (Hao Wu); Supervision, H.W. (Han Wang); Project Administration and Funding Acquisition, Z.S.

**Funding:** This work was supported by National Nature Science Foundation of China (Grant No. 61501225).

**Conflicts of Interest:** The authors declare no conflict of interest.

## References


1. Planck, M. *The Theory of Heat Radiation*; Dover: New York, NY, USA, 1991.
2. Fu, C.; Zhang, Z.M. Nanoscale radiation heat transfer for silicon at different doping levels. *Int. J. Heat Mass Transfer* **2005**, *49*, 1703–1718. [CrossRef]
3. Guha, B.; Otey, C.; Poitras, C.B.; Fan, S. Near-field Radiative Cooling of Nanostructures. *Nano Lett.* **2012**, *12*, 4546–4550. [CrossRef] [PubMed]
4. Basu, S.; Wang, L.P. Near-field radiative heat transfer between doped silicon nanowire arrays. *Appl. Phys. Lett.* **2013**, *102*, 053101. [CrossRef]
5. Park, Z.M.; Zhang, Z. Fundamentals and Applications of Near field Radiative Energy Transfer. *Front. Heat Mass Transfer* **2013**, *4*, 1083. [CrossRef]
6. Joulain, K.; Mulet, J.-P.; Marquier, F.; Carminati, R.; Greffet, J.-J. Surface electromagnetic waves thermally excited: Radiative heat transfer, coherent properties and Casimir forces revisited in the near heat. *Surf. Sci. Rep.* **2005**, *57*, 59–112. [CrossRef]
7. Shen, S.; Narayanaswamy, A.; Petersen, G. Surface Phonon Polaritons Mediated Energy Transfer between Nanoscale Gaps. *Nano Lett.* **2009**, *9*, 2909–2913. [CrossRef] [PubMed]
8. Francoeur, M.; Basu, S.; Petersen, S.J. Electric and Magnetic Surface Polariton Mediated Near field Radiative Heat Transfer between Metamaterials Made of Silicon Carbide Particles. *Opt. Express* **2011**, *19*, 18774–18788. [CrossRef] [PubMed]
9. Song, B.; Thompson, D.; Fiorino, A.; Ganjeh, Y.; Reddy, P.; Meyhofer, E. Radiative heat conductances between dielectric and metallic parallel plates with nanoscale gaps. *Nat. Nanotechnol.* **2016**, *11*, 509–514. [CrossRef] [PubMed]
10. St-Gelais, R.; Zhu, L.; Fan, S.; Lipson, M. Near-field radiative heat transfer between parallel structures in the deep subwacelength regime. *Nat. Nanotechnol.* **2016**, *11*, 515–519. [CrossRef] [PubMed]
11. Guo, Y.; Cortes, C.L.; Molesky, S.; Jacob, Z. Broadband super-Planckian thermal emission from hyperbolic metamaterials. *Appl. Phys. Lett.* **2012**, *101*, 131106. [CrossRef]
12. Chin, J.Y.; Steinle, T.; Wehlus, T.; Dregely, D.; Weiss, T.; Belotelov, V.I.; Stritzker, B.; Giessen, H. Nonreciprocal plasmonics enables giant enhancement of thinfilm Faradayrotation. *Nat. Commun.* **2013**, *4*, 1599. [CrossRef] [PubMed]
13. Messina, R.; Ben-Abdallah, P. Graphene-based photovoltaic cells for near-field thermal energy conversion. *Sci. Rep.* **2016**, *3*, 1383. [CrossRef] [PubMed]
14. Basu, S.; Zhang, Z.M.; Fu, C.J. Review of near-field thermal radiation and its application to energy conversion. *Int. J. Energy Res.* **2009**, *33*, 1203–1232. [CrossRef]
15. Park, K.; Basu, S.; King, W.P.; Zhang, Z.M. Performance analysis of near-field thermophotovoltaic devices considering absorption distribution. *J. Quant. Spectrosc. Radiat. Transfer* **2008**, *109*, 305–316. [CrossRef]
16. Wang, L.P.; Zhang, Z.M. Thermal rectification enabled by near-field radiative heat transfer between intrinsic silicon and other materials. *Nanoscale Microscale Thermophys. Eng.* **2013**, *17*, 337–348. [CrossRef]
17. Dransfeld, K.; Xu, J. The heat transfer between a heated tip and a substrate: Fast thermal microscopy. *J. Microsc.* **1988**, *152*, 35–42. [CrossRef]
18. Greenm, M.A. Time-asymmetric photovoltaics. *Nano Lett.* **2012**, *12*, 5985–5988. [CrossRef] [PubMed]
19. Gu, W.H.; Chang, S.J.; Fan, F.; Zhang, X.Z. InSb based subwavelength array for terahertz wave focusing. *Wuli Xuebao* **2016**, *65*, 010701.
20. Tabert, C.J.; Nicol, E.J. Valley-spin polarization in the magneto-optical response of silicone and other similar 2D crystals. *Phys. Rec. Lett.* **2013**, *110*, 197402. [CrossRef] [PubMed]
21. Wu, H.H.; Huang, Y.; Zhu, K.Y. Near field radiative transfer between magneto-dielectric uniaxial anisotropic media. *Opt. Lett.* **2015**, *40*, 4532–4535. [CrossRef] [PubMed]
22. Song, J.; Cheng, Q. Near-field radiative heat transfer between grapheme and anisotropic magneto-dielectric hyperbolic metamaterials. *Phys. Rev. B* **2016**, *94*, 125419. [CrossRef]
23. Basu, S.; Lee, B.J.; Zhang, Z.M. Near Field radiation calculated with an improved dielectric function model for doped silicon. *J. Heat Transfer* **2010**, *132*, 023302. [CrossRef]

24. Yang, Y.; Sabbaghi, P.; Wang, L. Effect of magnetic polaritons in SiC deep gratings on near field radiative transfer. *Int. J. Heat Mass Transfer* **2017**, *108*, 851–859. [CrossRef]
25. Wang, H.; Wu, H.; Zhou, J.Q. Nonreciprocal Optical Properties based on Magneto-optical materials: N-InAs, GaAs and HgCdTe. *J. Quant. Spectrosc. RA* **2018**, *206*, 254–259. [CrossRef]
26. Wang, H.; Wu, H.; Shen, Z.Y. Nonreciprocal optical properties of thermal radiation with SiC grating magneto-optical materials. *Opt. Express* **2017**, *25*, 19609–19618. [CrossRef] [PubMed]
27. Palik, E.D. *Handbook of Optical Constants of Solids*; Academic Press: San Diego, CA, USA, 1985; Volume 1.
28. Wang, H.; Liu, X.L.; Wang, L.P.; Zhang, Z.M. Anisotropic optical properties of silicon nanowire arrays based on the effective medium approximation. *Int. J. Therm. Sci.* **2013**, *65*, 62–69. [CrossRef]
29. Liu, X.L.; Zhang, R.Z.; Zhang, Z.M. Near field radiative heat transfer with doped-silicon nanostructured metamaterical. *Int. J. Heat Mass Transfer* **2014**, *73*, 389–398. [CrossRef]